ARTICLE IN PRESS

Energy xxx (2014) 1-15



Contents lists available at ScienceDirect

Energy

journal homepage: www.elsevier.com/locate/energy



Integration of industrial solar and gaseous waste heat into heat recovery loops using constant and variable temperature storage

Timothy G. Walmsley*, Michael R.W. Walmsley, Martin J. Atkins, James R. Neale

University of Waikato, Energy Research Centre, School of Engineering, Hamilton, Waikato, New Zealand

ARTICLE INFO

Article history: Received 23 December 2013 Received in revised form 26 January 2014 Accepted 28 January 2014 Available online xxx

Keywords: Heat recovery loop Low temperature heat recovery Solar heating Process integration

ABSTRACT

Solar is a renewable energy that can be used to provide process heat to industrial sites but require thermal storage. HRLs (heat recovery loops) are an indirect method for transferring heat from one process to another using an intermediate fluid. With HRL's thermal storage is also necessary to effectively meet the stop/start time dependent nature of the multiple source and sink streams. Combining solar heating with HRL's is a cost effective way to share common storage and piping infrastructure. The conventional HRL design method based on a CTS (constant temperature storage) and a new HRL design method using VTS (variable temperature storage) are applied to demonstrate the potential benefits of inter-plant heat integration and installing solar heating. The dairy case study had available 12 source streams including four spray dryer exhausts and six sink streams. The addition of the dryer exhausts as heat sources was a critical factor in gaining a heat recovery of 10.8 MW for the variable temperature storage design, of which 5.1 MW was contributed from exhaust heat recovery. For the same minimum approach temperature the VTS approach achieved 37% more heat recovery compared to the CTS approach. Solar heating also proved to be a valuable source to be integrated into an HRL with a pinch around the cold storage tank with the maximum addition of 0.9 MW of heating on average for the CTS approach and 1.0 MW of heating on average for the VTS approach.

© 2014 Elsevier Ltd. All rights reserved.

1. Introduction

Integration of renewable heat sources into chemical processes is increasingly becoming an area of intense research. Solar thermal stands out as viable candidate for providing heating to low pinch temperature processes. However solar heating is often uneconomic due to the large amount of infrastructure needed to ensure constant day and night heat supply. Where multiple low temperature semicontinuous processes are clustered on a single site, inter-plant heat integration may be effectively achieved using a HRL (heat recovery loop) as illustrated in Fig. 1. Heat storage, as a part of the HRL system, is needed to successfully meet the time dependent nature of the source and sink. Seeing that HRL's already have most of the infrastructure needed for solar heating there exists a nexus between the two concepts that may be utilised for their mutual advantage. Typically hot and cold storage temperatures in HRL's are fixed and the source and sink streams heat and cool the intermediate fluid between two storage temperature levels.

http://dx.doi.org/10.1016/j.energy.2014.01.103 0360-5442/© 2014 Elsevier Ltd. All rights reserved. Significant improvement in site heat recovery can be achieved through total site heat integration [1]. When low temperature semi-continuous processes, such as those found in dairy factories, are clustered into one large site, the opportunity exists for across plant indirect heat integration. Excess heat from one plant can be transferred to other plants with the aid of an intermediate fluid and thermal storage acting as a heat recovery loop (HRL) system [2] as shown in Fig. 1. Methods for designing indirect heat recovery systems for batch processes have been proposed by numerous authors, e.g. Refs. [3–5]. The methods apply almost exclusively to batch processes, but the principles also apply for semi-continuous processes especially when integrating across multiple plants on the same site [6].

Several recent studies by the authors have considered various parts of the design, operation and optimisation of HRL's including: thermal storage management options such as a stratified tank [7]; changes to storage temperature for seasonal production changes [8]; utilisation and sizing of thermal storage capacity [9]; characterisation of historical stream flow rates for HE (heat exchanger) area sizing [10]; and, the evaluation of different HE sizing methods through simulation of HRL performance for transient stream data [11]. Recently, Chen and Ciou [3] optimised an indirect heat

Corresponding author.

E-mail address: tgw7@waikato.ac.nz (T.G. Walmsley).

Nomenclature		cont	contribution
		1	limiting
Α	area (m²)	lc	cold storage
а	solar loss coefficient in Eq. (12)	lh	hot storage
C	heat capacity flow rate (kW/°C)	loop	loop stream
Н	enthalpy (kW)	h	hot
h	heat transfer film coefficient (kW/°C/m²)	ho	hot stream outlet
I	solar irradiance (kW/m²)	min	minimum
n	number	O	optical
NTU	number of (heat) transfer units	pro	process stream
n	exponent in Eq. (10)	r	recovery
Q	heat duty (kW)	S	supply or solar
Re	Reynolds number	sp	set point
T	temperature (°C)	t	target
U	overall heat transfer film coefficient (kW/°C/m²)	tot	total
ϵ	heat exchanger effectiveness		
η	efficiency	Abbreviations	
		CIP	clean-in-place
Subscri	ipts/superscripts	CTS	constant temperature storage
*	shifted	HE	heat exchanger
add	additional	HEN	heat exchanger network
amb	ambient	HRL	heat recovery loop
ave	average	PA	pinch analysis
c	cold stream	VTS	variable temperature storage
со	cold stream outlet		

recovery system for a batch process by allowing the target temperature set points of the intermediate fluid to differ for each HE resulting in a variable temperature storage system, which change offered improved heat recovery. In other areas, methods have been developed for maximising the integration of solar heating for low pinch temperature processes [12] and total site analysis [13]. However the economics of solar heating systems are often poor due to the infrastructure required to not only collect radiation heat, but also to store the heated fluid overnight. The integration of solar heating into an HRL is mutually beneficial because the HRL system provides the heat storage while solar is an additional heat source (Fig. 1).

Conventional control of an HRL is to measure and compare the outlet temperature of the loop fluid from each heat exchanger (HE) to a common hot or cold temperature set point. To achieve the set

point, the flow rate of the loop fluid through the HE is adjusted. An important characteristic of this approach is hot and cold storage temperatures are constant over time. An alternate approach to HRL control is to vary the set points of the HE's depending on their temperature driving force. This alternate approach is characterised by VTS (variable temperature storage) tanks due to mixing of different temperatures entering the tanks.

This paper aims to look at the effects of CTS (constant temperature storage) versus VTS operation of an HRL system with and without including solar as an additional heat source. The VTS approach has not been widely applied to HRLs, even though the possibility exists for improvements in indirect heat recovery from a simple operational change and the reallocation of some area. With this approach, the intermediate fluid flow rate is controlled to give an outlet temperature that is ΔT from the supply temperature of

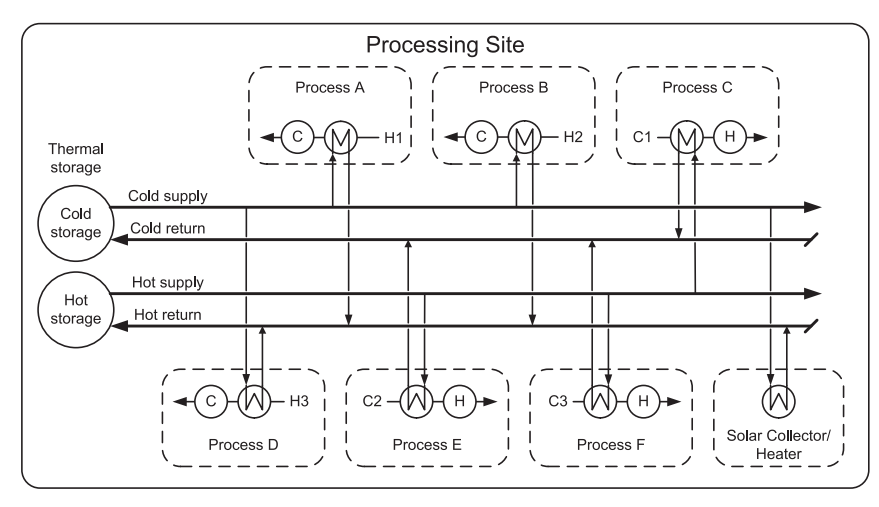


Fig. 1. Heat recovery loop network including the milk powder plant spray dryer.

selected source or sink streams on the loop. Over time the storage tank temperature and volume both vary depending on the thermal loads on the loop and the variability of the streams, which is modelled using the same spreadsheet tool applied by Walmsley et al. [11]. Solar heating may be added to an HRL to increase the quantity and upgrade the quality of heat storage depending on the location of the pinch temperature and the shape of the process Composite Curves.

2. Targeting, design and modelling methodologies for HRL's

2.1. Targeting and design methods for inter-plant heat integration via an HRL based on average data

In this section a graphical pinch based method for targeting inter-plant heat recovery across multiple semi-continuous plants is presented using a similar method to that proposed by Krummenacher and Favrat [5] for batch processes. Like traditional pinch analysis, the Composite Curves form an integral part of the targeting procedure. After zonal or intra-plant heat integration is targeted and heat exchanger networks are designed, streams that still require hot or cold utility are potential candidates for interplant integration at the total site level [1].

Inter-plant integration is complicated by the semi-continuous operation of dairy processes. A dairy process often has a number of different operating states such as on product, off product, and CIP (clean-in-place). Variations in production rate, process demand, and season also have an effect on the flow rate and temperature of some process streams. Walmsley et al. [11] demonstrated that an effective method for representing variable stream flow rates for designing an HRL is basing the design on daily time averaged flow rates, which include times in a day when a process is on, off or being cleaned, as opposed to the peak flow rates or median flow rates (Fig. 2). Time average values should only be taken across times when a plant is in regular operation. Daily time averaged stream data can then be used to draw hot and cold Composite Curves that show the daily average heating and cooling enthalpy deficits in each temperature range. How the Composite Curves are brought together and pinched is dependent on the operation - constant or variable temperature – of the storage system.

When targets are obtained from Composite Curves based on time average stream data, the target is for the daily average heat recovery. The targets assume intermediate loop fluid storage is continuously available, which is not always the case in practice. Composites Curves based on typical plant operating values may also be useful in understanding the real time balances between sources and sinks. Time averaged flow rates are lower than stream flow rates while on-product (often referred to as plant design values), therefore determining heat recovery targets from design flows often over predicts what can be recovered especially if there are streams with high flow rates but only operate for a few hours each day.

The algorithms for targeting and designing CTS and VTS HRL's have been developed and implemented into an Excel™ spreadsheet. This targeting and design tool is automated so that a wide range of designs may be generated based on time average stream data.

2.1.1. Constant temperature HRL storage design procedure

For the case of constant temperature storage, Composite Curves may be shifted by a full ΔT_{\min} or by $\Delta T_{\text{cont,pro}} + \Delta T_{\text{cont,loop}}$ since the heat recovery is indirect through an intermediate fluid. A pinch occurs between a limiting supply temperature of a stream and the opposite Composite Curve as shown in Fig. 3. The limiting supply temperature for the hot Composite Curve is the lowest supply temperature of a hot stream and the limiting supply temperature for the cold Composite Curve is the highest supply temperature of a cold stream. The limiting supply temperatures constrain the feasible storage temperature ranges for operating a CTS HRL. The supply temperatures of the streams forming the Composite Curves may be circled to clearly show when a pinch occurs. Once pinched, targets for indirect heat recovery may be calculated. The hot and cold storage temperatures can also be determined directly from the pinched Composite Curves, and a sloped line drawn to span the overlapping heat recovery region represents the average heat capacity flow rate of the HRL intermediate loop fluid. The pinched storage temperature (T_{lh}) is fixed while the other storage temperature (T_{lc}) may be varied within a small range without violating the ΔT_{\min} constraint. Assuming vertical integration between the hot and cold Composite Curves, T_{ho} is the outlet

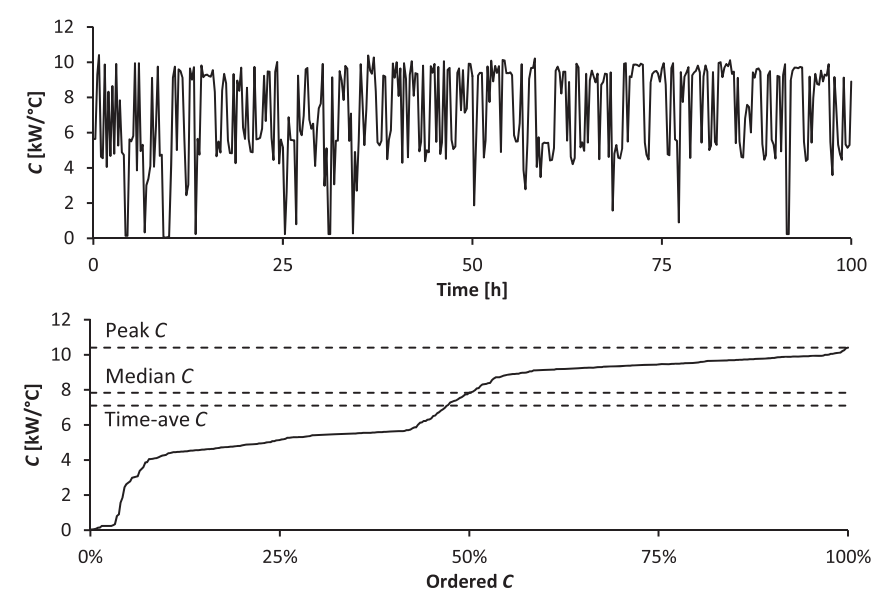


Fig. 2. Example raw and ordered heat capacity flow rate of a stream. Data taken from Walmsley et al. [11].

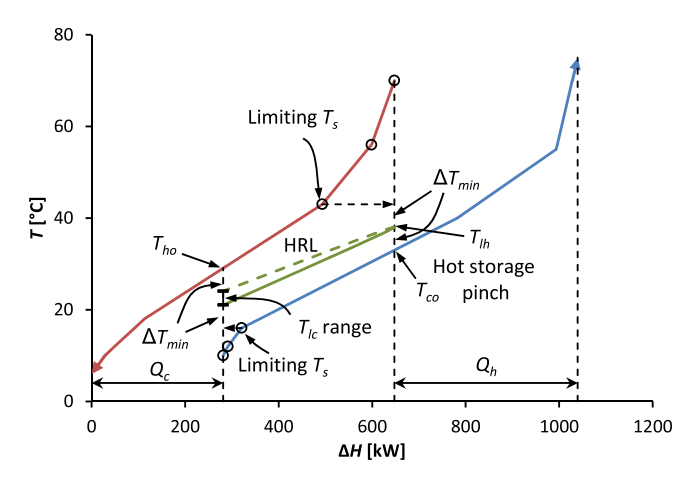


Fig. 3. Inter-plant Composite Curve for indirect heat recovery using an HRL with CTS. Steam data given in Walmsley et al. [11].

temperature of hot streams and T_{co} is the outlet temperature of the cold streams.

After identifying the HRL storage temperatures on the Composite Curve, heat exchanger areas are calculated using the time average stream data as was recommended by Walmsley et al. [11] for improved heat recovery per unit of area. For constant temperature storage operation, the storage temperatures become the control set-points for the outlet temperature of the loop fluid from heat exchangers on the HRL. Each heat exchanger in the HRL system receives fluid from one storage temperature and is controlled to return the fluid to the other storage tank at its temperature. Designs for a range of heat recovery levels are obtained by selecting new values for $\Delta T_{\rm min}$, which leads to new heat exchanger area requirements and new hot and cold storage temperatures.

A comprehensive example of this targeting and design method for HRL's with constant temperature storage is available in Chapter 20, authored by Walmsley et al., of the Handbook of Process Integration [14].

2.1.2. Variable temperature HRL storage design procedure

This section outlines a novel method for targeting and designing an HRL operated using a variable temperature storage system (Fig. 4). The approach is also based on the daily time-average Composite Curve and implemented into an ExcelTM spreadsheet.

The targeting and design procedure varies from traditional PA (pinch analysis) in that the cold Composite Curve is shifted under the hot composite curve by a selected feasible $Q_{\rm r}$. After $Q_{\rm r}$ is selected, the Composite Curves are shifted together to determine the minimum exchanger approach temperature, $\Delta T_{\rm min}$. In this method $\Delta T_{\rm min}$ and $\Delta T_{\rm cont}$ is no longer an input variable and therefore a modified method is needed to apply $\Delta T_{\rm cont}$ for different stream types to account for large differences in film coefficients between streams, e.g. gas versus liquid streams. Where necessary individual streams are shifted by $\Delta T_{\rm add}$ prior to the construction of the Composite Curve to penalise streams with poor heat transfer coefficients such that

$$T_{s(i)}^* = T_{s(i)} \pm \Delta T_{\text{add}} \tag{1a}$$

$$T_{\mathsf{t}(i)}^* = T_{\mathsf{t}(i)} \pm \Delta T_{\mathsf{add}} \tag{1b}$$

where the sign depends on whether the stream is a hot or cold stream. In this study, $\Delta T_{\rm add}$ for condensing vapour and liquid streams is zero since the respective heat transfer coefficients for these stream types are typically high whereas $\Delta T_{\rm add}$ for gaseous streams is 10 °C since gas streams normally have very low film coefficients [15]. This same approach for penalising gaseous streams, i.e. the dryer exhaust, may be applied in the CTS method. The Composite Curve is, therefore, partially shifted and the actual minimum approach temperature of a heat exchanger is $\Delta T_{\rm min} + \Delta T_{\rm add}$.

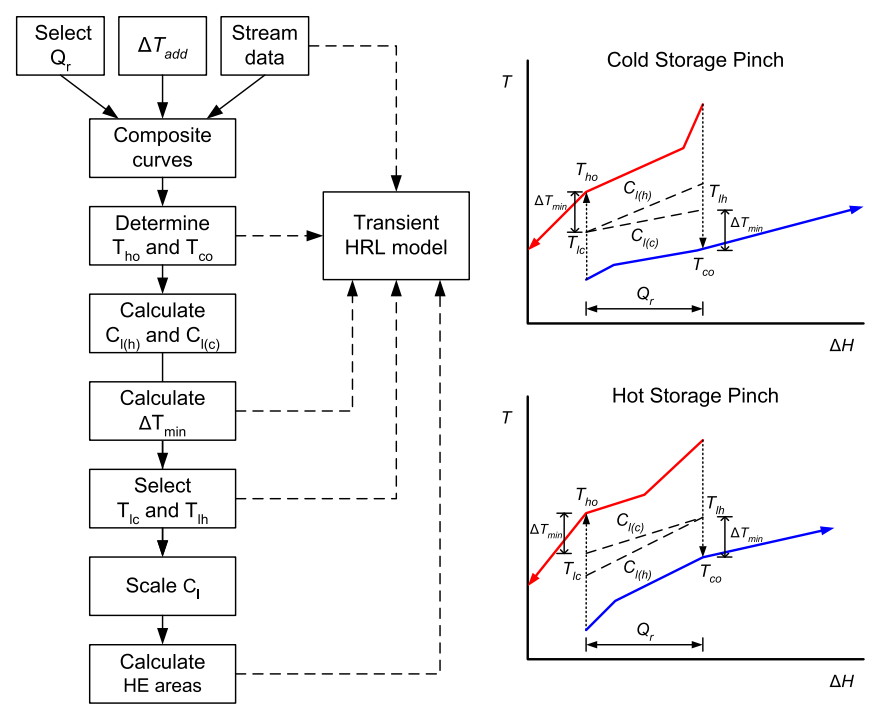


Fig. 4. Procedure for targeting and designing an HRL with VTS.

With the composite curves overlapping by Q_r , the hot stream outlet temperature, i.e. T_{ho} , and the cold stream outlet temperature, i.e. T_{co} , is determined assuming vertical heat integration as shown in Fig. 4. For the same heat recovery level these two outlet temperatures for the CTS and VTS methods are the same. Once these temperatures are found, the limiting combined loop flow rates based on the individual hot streams or the cold streams, i.e. $C_{\text{l(h)}}$ and $C_{\text{l(c)}}$, are calculated using

$$C_{l(h)} = \sum_{i=1}^{n_h} \frac{Q_i}{T_{s(i)}^* - T_{ho}}, \text{ where } Q_i = C_i(T_{s(i)}^* - \max(T_{ho}, T_{t(i)}^*))$$
(2a)

$$C_{l(c)} = \sum_{i=1}^{n_c} \frac{Q_i}{T_{co} - T_{s(i)}^*}, \text{ where } Q_i = C_i \Big(\min \Big(T_{co}, T_{t(i)}^* \Big) - T_{s(i)}^* \Big)$$
(2b)

where $n_{\rm h}$ is the number of hot streams and $n_{\rm c}$ is the number of cold streams. If $C_{\rm l(h)} < C_{\rm l(c)}$, then the pinch is at the cold storage whereas if $C_{\rm l(h)} > C_{\rm l(c)}$, then the pinch is at the hot storage. In some cases $C_{\rm l(h)} = C_{\rm l(c)}$ and both hot and cold storages are pinched. Streams that start outside the vertical overlapping region of the Composite Curves are not included in the calculation of the limiting heat capacity flow rate. The limiting hot and cold heat capacity flow rates define the minimum and maximum average flow rate boundaries for the VTS HRL system.

As demonstrated in Fig. 4, T_{ho} is related to T_{co} through ΔT_{min} and the minimum loop temperature difference,

$$T_{\rm co} + \Delta T_{\rm min} = T_{\rm ho} - \Delta T_{\rm min} + \Delta T_{\rm l.min} \tag{3}$$

where the minimum loop temperature difference is a function of the heat recovery level divided by the maximum limiting combined loop flow rate

$$\Delta T_{l,min} = \frac{Q_r}{\max(C_{l(h)}, C_{l(c)})}$$
(4)

These equations are rearranged to find an expression for ΔT_{\min} for a selected Q_r .

$$\Delta T_{\min} = \frac{1}{2} \left(T_{\text{ho}} - T_{\text{co}} + \frac{Q_{\text{r}}}{\max\left(C_{\text{l(h)}}, C_{\text{l(c)}}\right)} \right)$$
 (5)

The feasible range of average storage temperatures may be calculated using

$$T_{\text{co}} + \Delta T_{\min} \le T_{\text{lh}} \le T_{\text{ho}} - \Delta T_{\min} + \frac{Q_{\text{r}}}{C_{\text{l(h)}}}$$
 (6a)

for the hot storage temperature, T_{lh} , and

$$T_{\text{co}} + \Delta T_{\min} - \frac{Q_{\text{r}}}{C_{l(c)}} \le T_{lc} \le T_{\text{ho}} - \Delta T_{\min}$$
 (6b)

for the cold storage temperature, T_{lc} .

The designer may choose the average temperature of the non-pinched storage temperature within the range defined in the above equations. The selection may attempt to minimise total heat exchanger area or minimise the loop flow rate; or, one may simply take the mid-point temperature between the upper and lower temperature bounds. With the average storage temperatures ($T_{\rm lo}$ and $T_{\rm lc}$) and the outlet temperature of the process streams ($T_{\rm ho}$ and

 $T_{\rm co}$) decided, the combined average loop flow rate may be calculated

$$C_{l,ave} = \frac{Q_r}{T_{lb} - T_{lc}} \tag{7}$$

Focus is now given to the design of individual heat exchangers in the HRL system. For each heat exchanger, the inlet and outlet temperatures of the process stream and the hot and cold supply temperatures of the loop fluid have been determined. However, the flow rate of the loop through an individual exchanger is not yet known and nor is the outlet (return) temperature of the loop for an individual heat exchanger. As a result an additional equation is needed to fully define each heat exchanger. This equation is based on heat and mass flow rate conservation such that the loop flow rate through a heat exchanger is

$$C_{l(i)} = \frac{Q_i}{T_{s(i)}^* - T_{ho}} \left(\frac{C_{l,ave}}{C_{l(h)}}\right), \text{ where } i \in \text{hot streams}$$
 (8a)

$$C_{l(i)} = \frac{Q_i}{T_{co} - T_{s(i)}^*} \left(\frac{C_{l,ave}}{C_{l(c)}}\right), \text{ where } i \in \text{cold streams}$$
 (8b)

In the above equations, the heat capacity ratio provides a scaling factor for the limiting flow rate for an individual match. Applying the above equations ensure that the average heat and mass flow rates balance. Using the design heat capacity flow rate for a heat exchanger, the outlet/return temperature of the loop fluid may be calculated.

$$T_{\mathrm{l}(i),\mathrm{sp}} = T_{\mathrm{lh}} - \left(T_{\mathrm{s}(i)}^* - T_{\mathrm{ho}}\right) \frac{\mathsf{C}_{\mathrm{l}(\mathrm{h})}}{\mathsf{C}_{\mathrm{l}\,\mathrm{tot}}}, \text{ where } i \in \mathrm{hot\,streams}$$
 (9a)

$$T_{l(i),\text{sp}} = T_{lc} + \left(T_{co} - T_{s(i)}^*\right) \frac{C_{l(c)}}{C_{l,\text{tot}}}, \text{ where } i \in \text{cold streams}$$
 (9b)

This outlet temperature becomes a temperature set point for the control of the loop fluid through the exchanger. Each heat exchanger will have its own temperature set point returning fluid to the storage tank, which then mixes together. Hence, the HRL has a variable temperature storage system. With each heat exchanger fully defined, its area may be determined using the ε -NTU heat exchanger design equations [16]. All design parameters of the variable temperature storage HRL are now defined.

2.2. Method for transient modelling of actual heat recovery loop performance

An ExcelTM based spreadsheet tool has also been developed to simulate the transient performance of an HRL. The tool uses the loop temperature control set points and heat exchanger areas targeted from the steady state design to step-wise calculate the level and temperature of the hot and cold storage tanks. With historical or representative transient stream data, the model may be applied to estimate actual heat recovery for defined volumes of storage. When a stream falls short of its target temperature or storage is unavailable, utility is consumed. In the model, the capacity of the storage tanks and intermediate fluid properties such as density and heat capacity may be specified and the storage tank is assumed to be well-mixed. In this work, the intermediate fluid is water and the effect of storage capacity is investigated.

For this case study the model solves nearly 140,000 countercurrent heat exchanger problems. Each problem has an unknown loop heat capacity flow rate, process stream outlet temperature and heat duty. Inlet loop temperatures to the heat exchanger are the same as the storage temperature from where it is withdrawn. Outlet loop temperatures are the control set point, which is specified in the design. Dynamics relating to process control are not modelled in the spreadsheet. Given a heat exchanger area and overall heat transfer coefficient (U), the heat exchanger problems become fully defined. However to calculate the unknowns neither the $\Delta T_{\rm LM}$ (log-mean-temperature-difference) nor the ε -NTU method may be applied. The $\Delta T_{\rm LM}$ method requires the temperatures in and out of the heat exchanger to be defined; whereas the ε -NTU method requires both heat capacity flow rates to be known. Hence an iterative approach was implemented and a generalised solutions table (600×600) was generated by iteratively solving a simple, single heat exchanger model. Looking up the solution on the table then enabled the HRL model to solve quickly in about 1 min avoiding the need to iteratively solve thousands of heat exchanger problems, which takes a few hours. To simplify the problem, all heat exchangers, regardless of type, are modelled as a counter current heat exchanger. Cross-flow heat exchangers applied to transfer heat to/from gaseous streams from/to liquid streams normally have multiple liquid passes (>6) to produce a near counter flow arrangement [16].

Fluctuations in process stream flow rates and temperature, which are characteristic of semi-continuous processes, are successfully accounted for in the spreadsheet model. Heat exchanger areas are designed according to the time-average flow rate of the process stream. When the flow rate of a stream falls below the design point flow rate, U and Q are reduced, and when the flow rate is above, U and Q increase. To account for this in the modelling, individual U values are calculated from the corresponding film coefficients (h) for the process and loop streams as a function of Reynolds number (Re). Liquids are assigned a design film coefficient of $4000 \, \text{W}/^{\circ} \text{C/m}^2$; vapours are assigned $2400 \, \text{W}/^{\circ} \text{C/m}^2$; and gaseous flows are $71 \, \text{W}/^{\circ} \text{C/m}^2$. Assuming the fluids have a constant viscosity, density, and heat capacity, the ratio of the instantaneous h to the design h_{dp} is related to the ratio of C through the Reynolds number, where a and b are constants specific to a heat exchanger design,

$$h = a \cdot Re^n \Rightarrow \frac{h}{h_{\rm dp}} = \left(\frac{Re}{Re_{\rm dp}}\right)^n \cong \left(\frac{C}{C_{\rm dp}}\right)^n$$
 (10)

The spreadsheet model developed for the transient study uses a value of 0.58 for n, which is specific to a plate heat exchanger [17] but is not out of the range of values for finned tube heat exchangers, 0.52-0.70, calculated from the correlations of Kays and London [16]. Constant a may be slightly dependent on fluid properties such as the Prandtl number, which is a function of temperature. In this work, a is assumed to be constant, as is often the case for liquids with relatively small temperature changes. Design point values are based on the average operating flow rate of a stream. Again, to

avoid an iterative solution, a value for h of the loop side of the heat exchangers was required without first knowing the duty of the heat exchanger and $C_{l(i)}$. As a result, the loop side flow rate was approximated by

$$\frac{C_{l(i)}}{C_{pro(i)}} \stackrel{=}{=} \frac{C_{l(i),dp}}{C_{pro(i),dp}}$$
(11)

for the calculation of h and then U. In a simple test case, the difference between the estimated and calculated loop C values was found to be at most 3%.

Included in the HRL model is solar heating based on recorded data from a local weather station. Solar collector efficiency and duty has been modelled using the design equations and constants given by Atkins et al. [12].

$$Q_{s} = A_{s} \Big(\eta_{0} I - a_{1} (T_{s} - T_{amb}) - a_{2} (T_{s} - T_{amb})^{2} \Big)$$
 (12)

where Q_s is the solar heating duty, η_0 is the optical efficiency (0.764), A_s is the area of the solar collector, I is the solar irradiance, a_1 (1.53 kW/m²/°C) and a_2 (0.0003 kW/m²/°C²) are thermal loss coefficients, T_s is the average temperature of the collector, and T_{amb} is the ambient temperature.

2.3. Principles for integrating solar heating with HRL's

The integration of solar heating with HRL's is logical because both systems need thermal storage to account for their variable heat supply/demand throughout a day/night cycle. Fig. 5 illustrates the effect of integrating solar heating into two general cases, which may be characterised by the location of the pinch.

In the first case (Fig. 5a) the pinch is at the CS (cold storage) temperature indicating a lack of heat sources. As a result solar heating may be integrated as an additional heat source and either CTS or VTS control may be applied to operate the HRL. It is advantageous to further increase the area of the sink heat exchangers to ensure that the extra heating from solar is fully utilised by the HRL.

The second case (Fig. 5b) is where the pinch is located around the hot storage temperature. Applying solar heating to produce hot water at the pinched hot storage temperature for CTS operation is totally ineffective and inappropriate. This is analogous to adding a hot utility to below the pinch temperature. For VTS operation with a hot storage pinch, the addition of solar heating is like adding a hot utility across the pinch that increases the site's required cooling duty but decreases the site's heating load. To generate benefits from adding solar, the HRL fluid temperature needs to be raised above the pinch temperature and some modifications to the HRL design

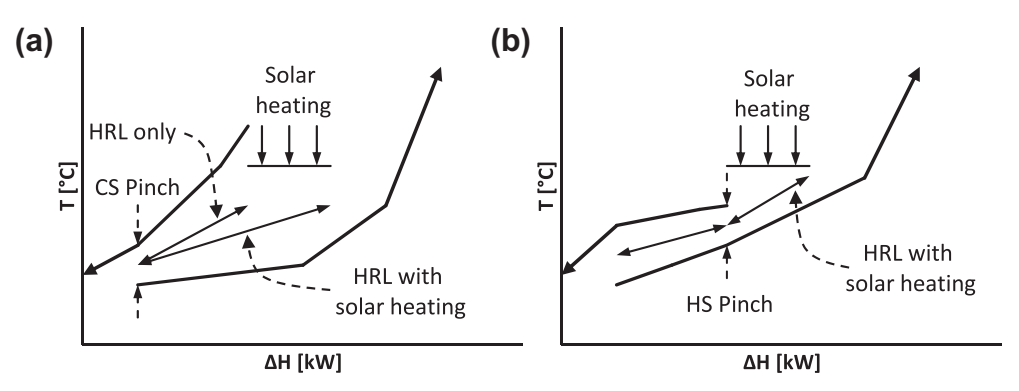


Fig. 5. Composite Curves for the integration of solar heating with HRL's for processes with cold storage pinch (a) and hot storage pinch (b).

may need to be made such as adding a third storage tank with the temperature level as indicated in Fig. 5b.

3. Data collection and characterisation

Stream data for four milk powder plants, four other dairy processes, site hot water and two utility units (e.g. compressor) have been obtained from a New Zealand dairy factory for a period of two months during peak processing at intervals of 10 min. Volumetric flow rates were measured by magnetic flow meters and recorded by the company's computer system whereas most temperatures were measured but not logged. As a result historical average temperatures have been used in most cases.

Table 1 presents the stream data for the 18 process streams with the addition of a solar collector. Operating average and daily time average heat capacity flow rates are calculated and temperatures are averaged for while a stream is in operation. The daily time average values include periods when a stream is unavailable throughout a normal day's plant operation due to cleaning and off-product times. Duties based on both heat capacity flow rates are also presented. The solar collector is assigned a supply temperature of 85 °C, and it is assumed that solar heating can heat the intermediate fluid up to 80 °C in evacuated tubes.

Some streams such as the condenser have a high operational duty (993 kW) but only operate for around 8 h/d resulting in a time average duty of 351 kW. The condenser duty is plotted in Fig. 6 using instantaneous values for a 72 h period and ordered values for the entire two months. On the other hand, streams like site hot water are continuously available but its supply temperature and flow rate fluctuates noticeably as shown in Fig. 7.

Solar irradiance and ambient temperature data recorded at a nearby weather station has been downloaded from New Zealand's National Climate Database [18]. Solar irradiance data for the entire two months is plotted in Fig. 8 using time of day as the *x*-axis and showing the day average (0.43 kW/m²), day/night average (0.25 kW/m²) and the average of the daily peak (0.97 kW/m²).

4. Steady state HRL targets and design

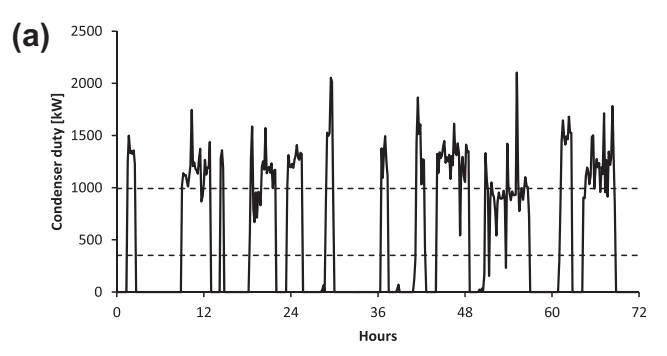
4.1. Site composite curves

The site's heating and cooling demand profiles may be determined using the stream data in Table 1 as shown in Fig. 9. The dryer

 Table 1

 Extracted stream data including the spray dryer exhaust and solar heating.

Stream	Туре	T_{s} [°C]	$T_{\rm t} [^{\circ} {\sf C}]$	Operating		Time-average	
				<i>C</i> [kW/°c]	Q [kW]	<i>C</i> [kW/°C]	Q [kW]
Dryer exhaust A	Hot	75	55	143	2,851	139	2,785
Dryer exhaust B	Hot	75	55	75	1,497	73	1,462
Dryer exhaust C	Hot	75	55	45	898	44	877
Dryer exhaust D	Hot	75	55	29	570	28	557
Utility unit A	Hot	45	30	10	146	8	120
Utility unit B	Hot	45	30	10	146	8	120
Casien A	Hot	50	20	33	999	22	647
Casien B	Hot	50	20	49	1,477	32	956
Casien C	Hot	50	20	49	1,485	32	962
Condenser	Hot	80	79	993	993	351	351
Cheese A	Hot	35	20	120	1,797	98	1,470
Cheese B	Hot	35	20	139	2,074	114	1,691
Solar collector	Hot	85	_	_	_	_	_
Site hot water (SHW)	Cold	16	65	160	7,827	160	7,827
Milk treatment A	Cold	10	50	104	4,159	104	4,159
Milk treatment B	Cold	10	50	104	4,159	104	4,159
Milk treatment C	Cold	11	50	116	4,563	116	4,563
Whey A	Cold	12	45	20	663	16	522
Whey B	Cold	14	45	11	340	9	267



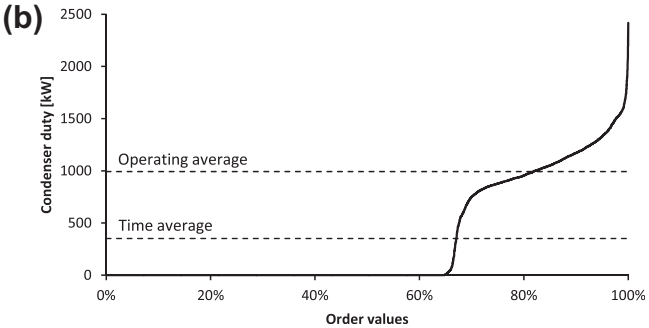
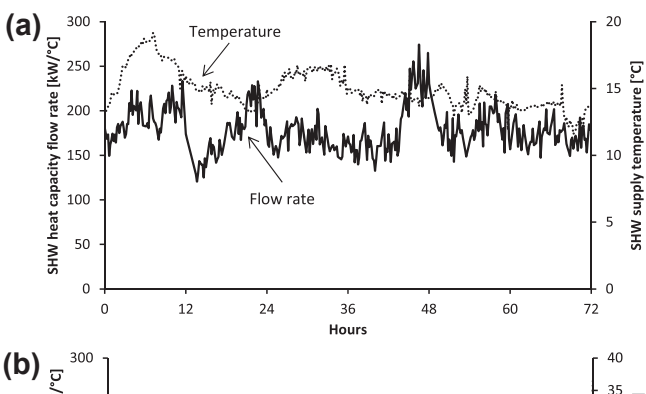


Fig. 6. Condenser duty for a 72 h period (a) and as ordered values for the entire two months (b).

exhaust stream has been shifted by 10 °C to reflect its lower heat transfer film coefficient compared to other liquid and condensing vapour streams. The total heating requirement is 21.5 MW on average and the total cooling requirement is 12.0 MW on average.

4.2. Average heat recovery targeting for CTS

Average inter-plant heat recovery achieved by CTS HRL is targeted using a ΔT_{min} of 5 °C. As a rule of thumb, liquid/liquid heat



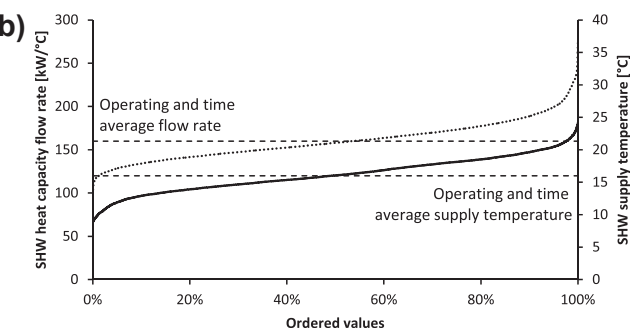


Fig. 7. Site hot water supply temperature and heat capacity flow rate for a 72 h period (a) and as ordered values for the entire two months (b).

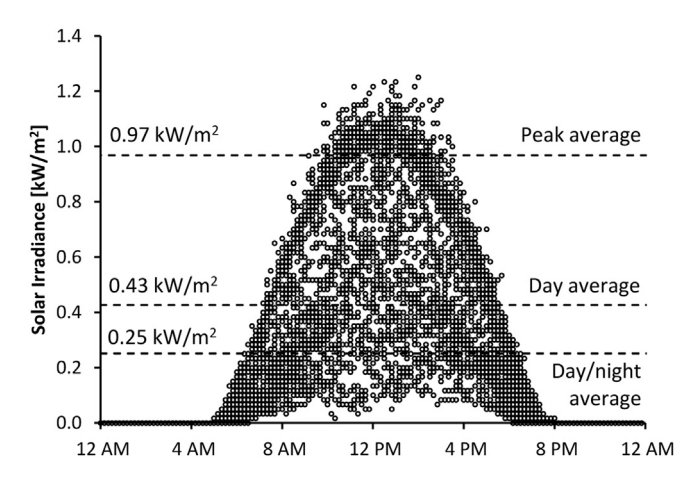


Fig. 8. Solar irradiance recorded by closest weather station the dairy factory [18].

recovery using plate heat exchangers tend to be economic at a $\Delta T_{\rm min}$ of 5 °C as was demonstrated by Walmsley et al. (2013) for a stand-alone milk powder plant. Fig. 10 presents the pinched Composite Curves for targeting a CTS HRL showing a heat recovery of 8.3 MW. The pinch is around the cold storage temperature caused by site utility unit A's and B's common supply temperatures.

Cheese A and B have been removed from the analysis and the Composite Curve in Fig. 10 to increase heat recovery for a $\Delta T_{\rm min}$ of 5 °C. Cheese A and B have the lowest hot stream supply temperature and leaving these streams in the analysis would limit heat recovery to a maximum of 7.5 MW. Above a heat recovery of 7.5 MW, streams Cheese A and B would be encompassed in the overlap region of the Composite Curves causing a hot storage pinch and a $\Delta T_{\rm min}$ of less than 5 °C. In general, the stream causing a pinch is removed, which sometimes allows the composite curves to be further overlapped indicating increased heat recovery.

There is a small range of feasible temperatures for the non-pinched hot storage temperature. The effect of varying the hot storage temperature on total area and the loop flow rate is shown in Fig. 11. At the hottest feasible hot storage temperature, the loop flow rate, pressure drop and pumping costs are minimised; whereas

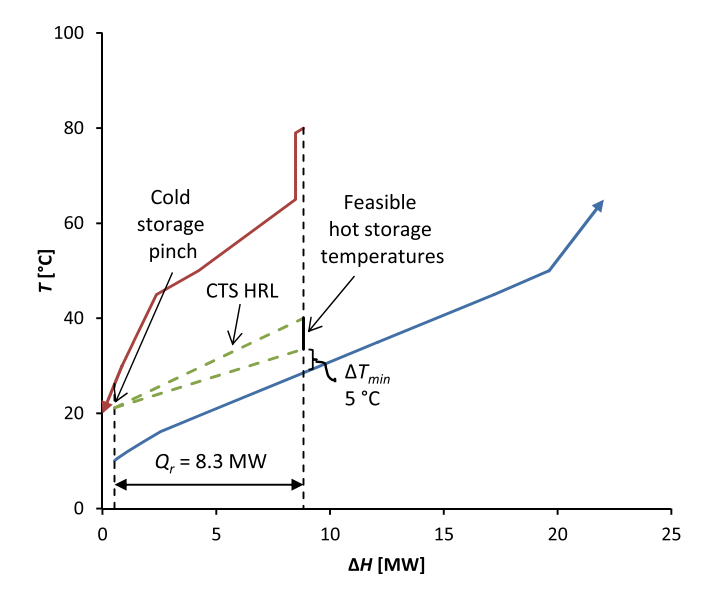


Fig. 10. Heat recovery targeting for CTS based on a ΔT_{min} of 5 °C. Cheese A and B removed from analysis.

different cold storage temperature minimises total area. From experience, minimising the loop flow rate produces a more practical solution in terms of loop temperature difference and flow rate whereas optimising for the minimum area tends to make less of an impact as indicated by the flatness of the total area curve.

4.3. Average heat recovery targeting for VTS

A heat recovery target for a VTS HRL is determined assuming a $\Delta T_{\rm min}$ of 5 °C as shown in Fig. 12. The heat recovery target for the VTS approach is 11.3 MW, which is considerably higher than CTS approach. Fig. 13 presents the effect of hot storage temperature selection where minimising area is at odds with minimising loop flow rate. The CTS method can also recover 11.3 MW, although it requires a lower $\Delta T_{\rm min}$ of 0.2 °C and hence a much larger total heat transfer area. To better compare between the

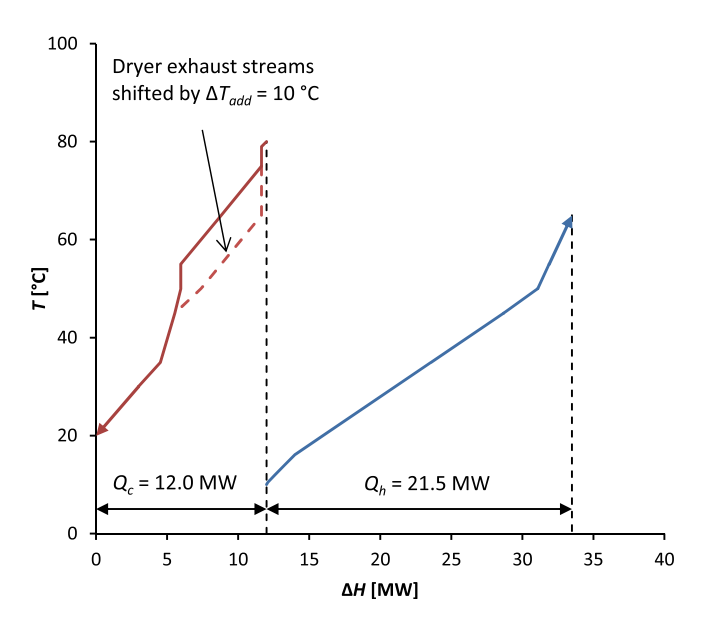


Fig. 9. Time average Composite Curves of available streams for the HRL. Solar heating is not included.

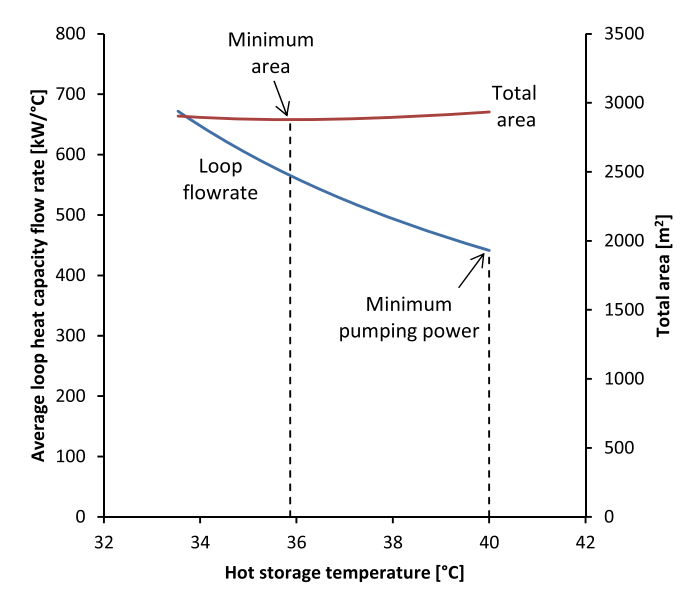


Fig. 11. Effect of cold storage temperature selection on total area and loop flow rate for a CTS HRL based on a ΔT_{\min} of 5 °C.

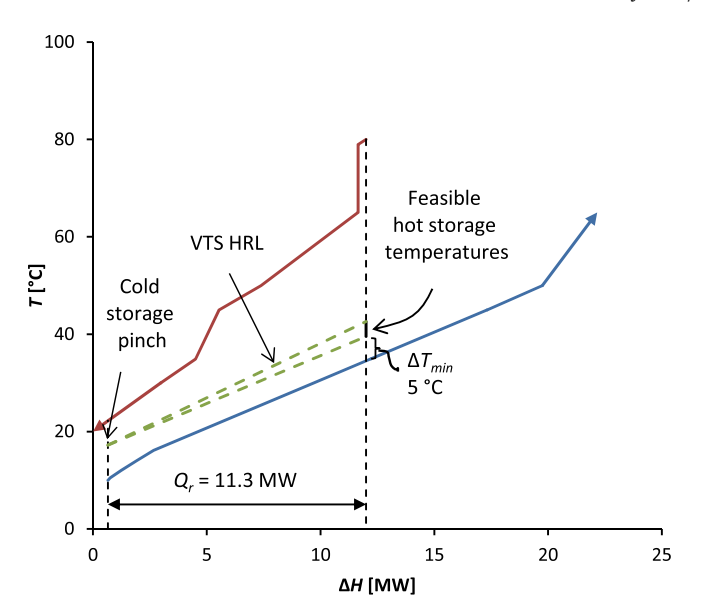


Fig. 12. Heat recovery targeting for VTS based on a ΔT_{\min} of 5 °C.

two methods, an understanding of the trade-off between heat recovery, total area and average loop flow rate across a boarder range is needed.

4.4. Heat recovery, total area and loop flow rate trade-off

In designing an HRL there is an acute trade-off between heat recovery, total area and the loop flow rate. Heat recovery delivers utility savings, heat exchanger area is a capital cost and the loop flow rate determines the pressure drop and pumping costs. The heat recovery performance of CTS and VTS HRL's is compared for a range of $\Delta T_{\rm min}$ values in Fig. 14. In general the VTS method more effectively distributes temperature driving forces between heat exchangers resulting in higher $\Delta T_{\rm min}$ values compared to the CTS method. Discontinuities in this graph as well the other graphs in this section are caused by streams being added or removed from the HRL design. For a $\Delta T_{\rm min}$ of 5 °C, the VTS

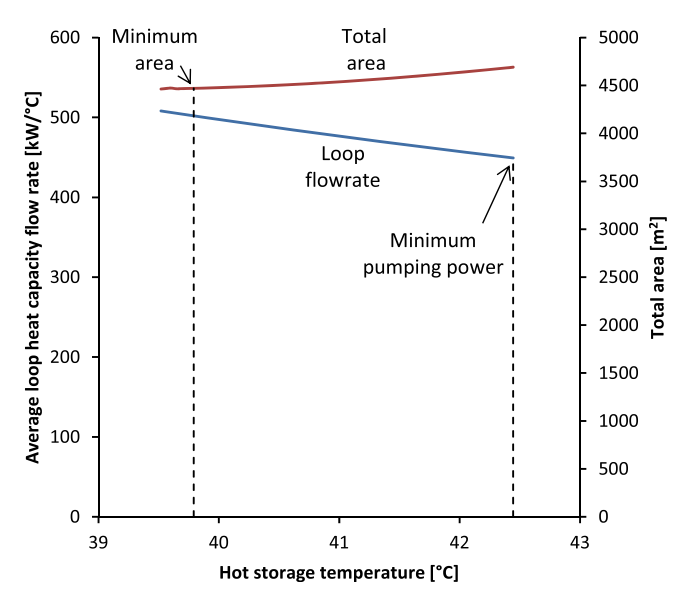


Fig. 13. Effect of cold storage temperature selection on total area and loop flow rate for a VTS HRL based on a ΔT_{\min} of 5 °C.

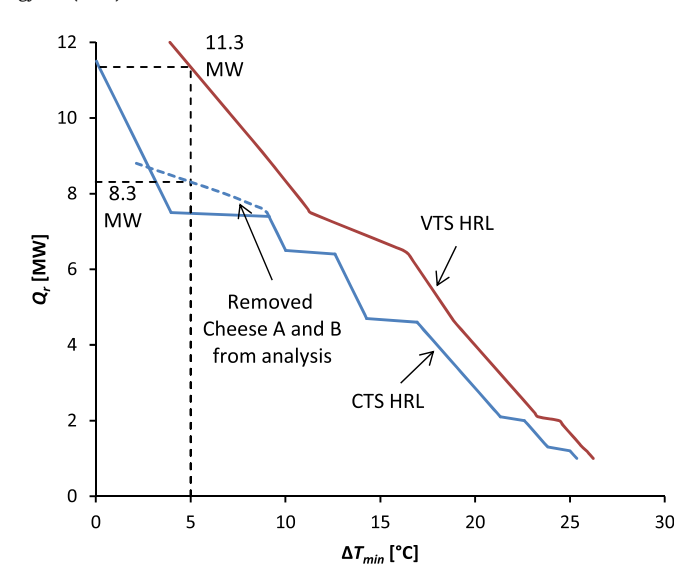


Fig. 14. Heat recovery versus minimum approach temperature.

approach recovers 11.3 MW of heat compared to 8.3 MW for the CTS design.

The heat recovery performance may also be plotted against total network area including the dryer exhaust heat exchanger area as shown in Fig. 15 and total network area excluding the dryer exhaust heat exchanger area as shown in Fig. 16. Black dotted lines are included that correspond to a $\Delta T_{\rm min}$ of 5 °C for the two design approaches. Below 9.9 MW of heat recovery the CTS approach for this problem provides better heat recovery per unit of area while the VTS approach is advantageous above 9.9 MW of heat recovery if the dryer exhaust area is included. The maximum inter-plant heat recovery for the site, 12.0 MW, is feasible to achieve using the VTS method with a $\Delta T_{\rm min}$ of 3.9 °C, at which heat recovery level the Composite Curves for a threshold problem. The CTS storage has a maximum heat recovery of 11.5 MW with $\Delta T_{\rm min}$ approaching zero.

The lower total area achieved by the CTS method below 9.9 MW of heat recovery is mostly due to lower inlet and outlet loop temperatures for the dryer exhaust heat exchangers. The lower

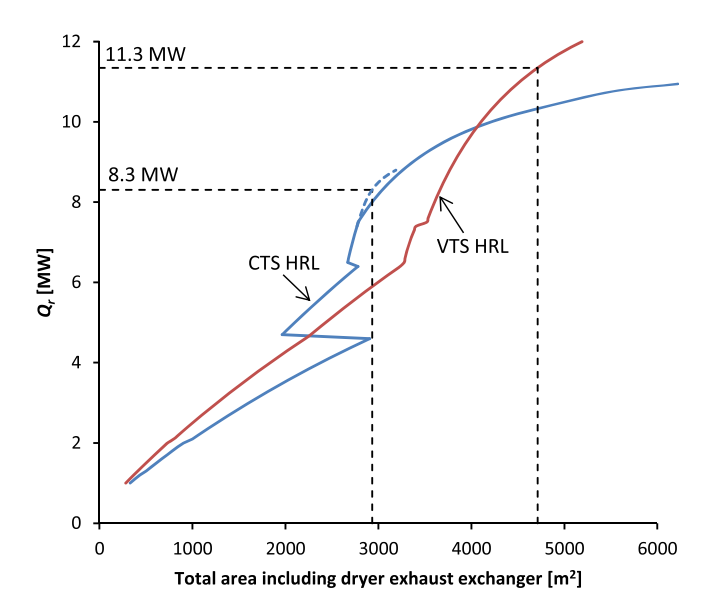


Fig. 15. Heat recovery versus total area including the dryer exhaust exchanger.

Please cite this article in press as: Walmsley TG, et al., Integration of industrial solar and gaseous waste heat into heat recovery loops using constant and variable temperature storage, Energy (2014), http://dx.doi.org/10.1016/j.energy.2014.01.103

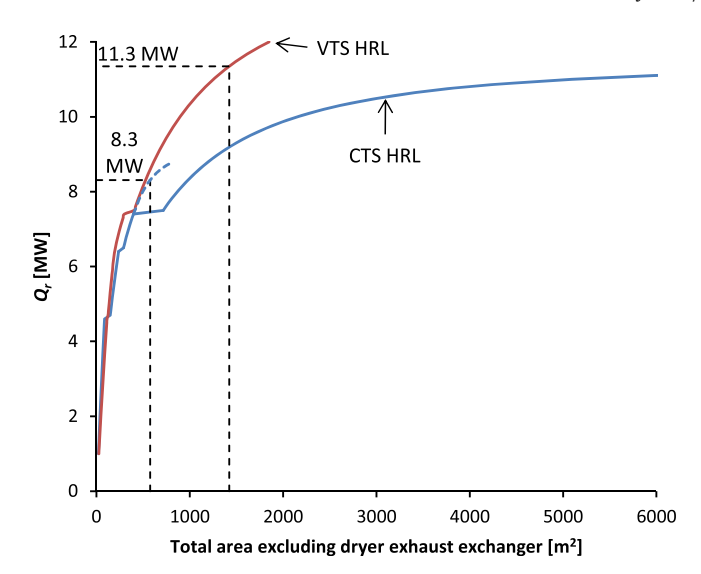


Fig. 16. Heat recovery versus total area excluding the dryer exhaust exchanger.

loop temperatures for the CTS design improve the temperature driving force of heat exchangers on the hot side of the loop, which includes the dryer exhaust exchangers. At 9.9 MW of heat recovery the area required for dryer exhaust heat recovery comprises 50% of the total HRL system area, which percentage is higher for heat recovery targets less than 9.9 MW. As a result heat recovery is plotted against the total area excluding the dryer exhaust heat exchangers as presented in Fig. 16. This graph provides a different perspective on which design approach is better. In Fig. 16, the VTS system gives substantially improved heat recovery per unit area for heat recovery greater than 7.5 MW. Below a heat recovery of 7.5 MW, the total area is dominated by the area required for dryer exhaust heat recovery. As a result the CTS approach in Fig. 15 appears to be better at the design stage due to lower loop temperatures maximising the temperature driving force for the dryer exhaust exchanger.

The temperature difference between the hot and cold loop temperatures is a key factor affecting the required loop flow rate (Fig. 17). Small temperature differences require large loop flow rates. When selecting the non-pinched storage temperature, the philosophy has been to minimise the loop flow rate, thus minimising pressure drop and pumping costs. Several additional curves for both CTS and VTS methods could be generated by selecting different non-pinched storage temperatures. When targeting site heat recovery below 5.2 MW, it is possible to remove the stream with the limiting supply temperature from the analysis and improve the final design. As a result Cheese A and B are removed for the CTS design to show this effect while also being able to achieve a $\Delta T_{\rm min}$ of 5 °C.

4.5. Integration of solar heating into the HRL design

The integration of solar heating with an HRL is beneficial when the pinch is around the cold storage temperature, which is the case for the CTS and VTS methods with a $\Delta T_{\rm min}$ of 5 °C. In this section, the maximum and practical integration of solar heating into the 5 °C $\Delta T_{\rm min}$ solutions is investigated.

Fig. 18 shows the maximum amount of solar heat that can be integrated into the CTS HRL without violating the $\Delta T_{\rm min}$ constraint whereas Fig. 19 is for a VTS HRL. For these cases the pinch at the hot storage tank is caused by the solar heating. For the CTS approach, the hot storage pinch is between the supply temperature of utility

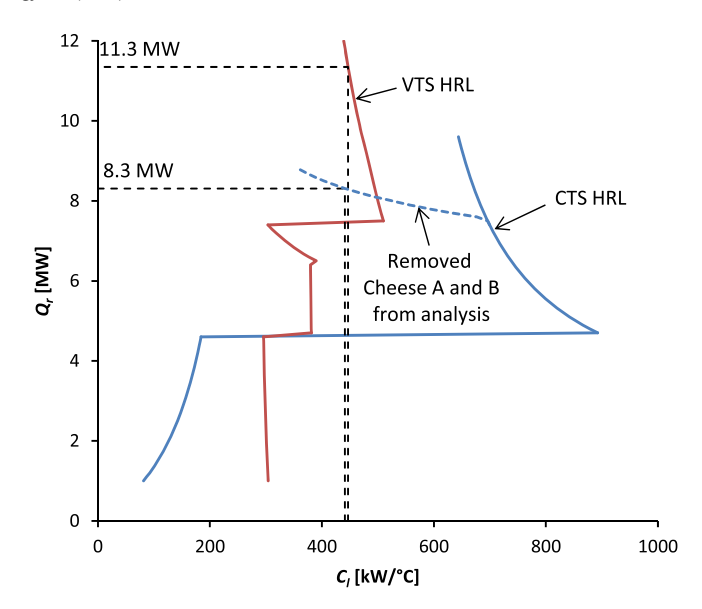


Fig. 17. Heat recovery versus heat capacity flow rate of the loop.

units A and B and the cold Composite Curve as a result of adding solar to the HRL. For the VTS approach, the second pinch is related to the limiting heat capacity flow rate of the loop based on the hot and cold streams, i.e. $C_{l(h)}$ and $C_{l(c)}$. For a second pinch to occur it is necessary that $C_{l(h)} = C_{l(c)}$, where $C_{l(h)}$ includes solar heating as a hot stream and $C_{l(c)}$ is based on T_{co} after solar heating.

Achieving the maximum integration of solar heating is impractical due to the daily solar heating cycle requiring excessive thermal storage. By analysing the solar irradiance data it is found that 65% of the day/night cycle is below the day/night irradiance average of 0.25 kW/m². To account for the cyclic nature of solar availability an estimated 3000 m³ of thermal storage is required whereas storage for an HRL is typically less than 500 m³. If the outlet temperature of the solar collector was higher than 85 °C, which is the value used in this work, the amount of required storage could be lessened. There is an acute optimisation between solar collector temperature, collector heat loss and storage needs that may be analysed as part of future work.

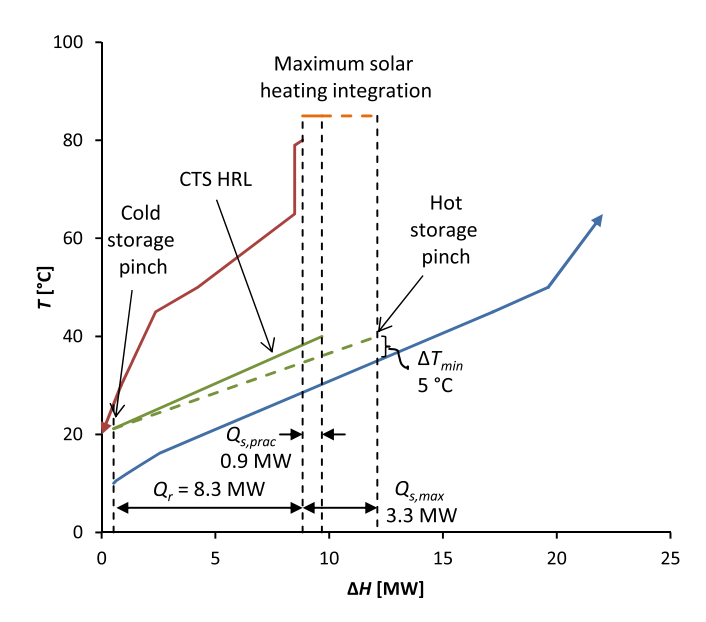


Fig. 18. Maximum and practical average heat recovery and solar heating targets for a CTS HRL based on a $\Delta T_{\rm min}$ of 5 °C.

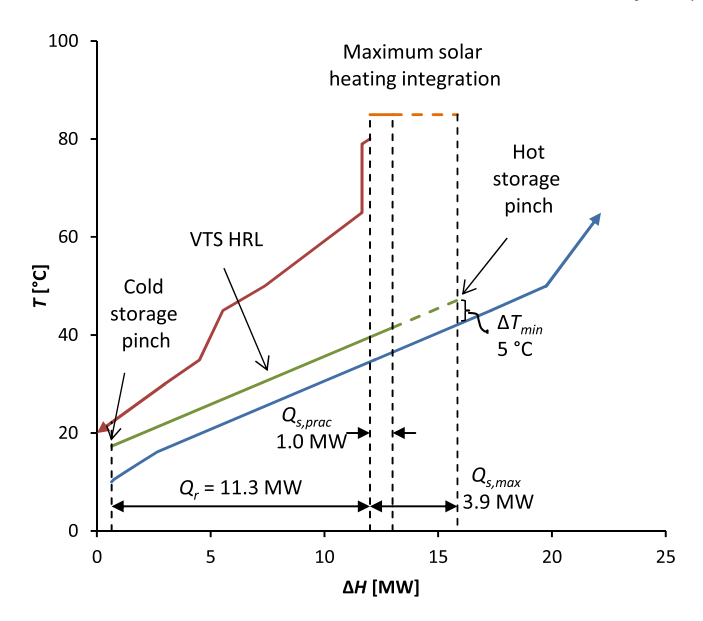


Fig. 19. Maximum and practical average heat recovery and solar heating targets for a VTS HRL based on a $\Delta T_{\rm min}$ of 5 °C.

A practical amount of solar heating that requires minimal storage can be calculated from $Q_{s,max}$ assuming that $Q_{s,max}$ is obtained by the daily average peak solar irradiance, for which there is sufficient sinks on average. As a result this maximum duty is scaled down by the ratio of day/night average to daily average peak solar irradiance (I) to obtain a practical average duty of solar heating.

$$Q_{s,prac} = Q_{s,max} \frac{I_{s,ave}}{I_{s,peak}}$$
 (13)

The practical amount of solar heating is estimated as 0.9 MW for the CTS design and 1.0 MW for the VTS design.

Solar heating duty is a function of the collector area. If the solar collector size is based on the day/night solar irradiance average of 0.25 kW/m², the collector would have insufficient area to achieve the desired average heating duty because the average irradiance value does not take into account the optical and heat losses of the collector. Preliminary analysis of the solar collector suggests that one square meter can average 0.178 kW for the day/night cycle. Without correctly taking into account optical and thermal losses the solar collector would be undersized by 30% for this case and unable to meet its expected design duty. The solar collector needs to be 4776 m² for the CTS design and 5606 m² for the VTS design.

4.6. Maximum energy recovery HRL designs

The design of an HRL requires the specification of heat exchanger areas and temperature control set points for the return temperature of the loop fluid to storage as provided in Table 2. These design values provide the details for the four HRL designs modelled using transient data. Other parameters such as the operating temperature of the storage units and the loop flow rate may be determined from these two specifications. Heat exchanger areas are sized based on the time average flow rate. Maximum heat recovery HRL designs are targeted to recover 8.3 MW for the CTS design and 11.3 MW for the VTS design with the option of integrating solar heating.

Table 2 HRL design specifications.

Stream	Loop temperature return set point [°C]			Area [m ²]				
	CTS	CTS with solar	VTS	VTS with solar	CTS	CTS with solar	VTS	VTS with solar
Hot streams								
Dryer exhaust A	40.0	40.0	60.0	60.0	1,156	1,156	1,613	1,613
Dryer exhaust B	40.0	40.0	60.0	60.0	607	607	847	847
Dryer exhaust C	40.0	40.0	60.0	60.0	364	364	508	508
Dryer exhaust D	40.0	40.0	60.0	60.0	231	231	323	323
Utility unit A	40.0	40.0	40.0	40.0	9	9	7	7
Utility unit B	40.0	40.0	40.0	40.0	9	9	7	7
Casien A	40.0	40.0	45.0	45.0	36	36	60	60
Casien B	40.0	40.0	45.0	45.0	53	53	89	89
Casien C	40.0	40.0	45.0	45.0	53	53	89	89
Condenser	40.0	40.0	75.0	75.0	5	5	10	10
Cheese A	40.0	40.0	29.9	29.9	0	0	125	125
Cheese B	40.0	40.0	29.9	29.9	0	0	144	144
Solar collector	40.0	40.0	80.0	80.0	0	4,776	0	5,606
Total HE area					2,523	2,523	3,822	3,822
Cold streams								
Site hot water	21.2	21.2	21.7	21.6	127	158	219	257
Milk treatment A	21.2	21.2	14.7	14.8	85	100	205	230
Milk treatment B	21.2	21.2	14.7	14.8	85	100	205	230
Milk treatment C	21.2	21.2	15.3	15.3	94	111	221	249
Whey A	21.2	21.2	17.0	17.0	13	15	28	32
Whey B	21.2	21.2	19.2	19.2	7	8	14	16
Total HE area					411	494	890	1,013

5. Transient modelling of HRL performance

5.1. HRL performance with 500 m³ storage tanks

At any instance the combined heat recovery from the sources may not exactly match the combined heat transfer to the sinks. When that occurs there is a hot and cold imbalance. Most imbalances are short term only lasting for a couple of hours but it is possible that a long term imbalance is sustained for days when plants cease to run due to a lack of milk production from the farms. Short term imbalance is accommodated for by sizing sufficient thermal storage capacity in the HRL system. Long term imbalance results in one of the storage tanks becoming completely empty of fluid.

The instantaneous storage level and hot and cold storage temperatures across a 14 day period is presented in Fig. 20 for the CTS design, Fig. 21 for the CTS with solar design, Fig. 22 for the VTS design and Fig. 23 for the VTS with solar design. These plots demonstrate the real-time transient behaviour of dairy process streams and their associated heating and cooling demands impacting on the HRL operation. Even with 500 m³ of thermal storage the hot storage tank can quickly fill or empty depending on the mix of streams available. The amount of thermal storage is related to the temperature difference of the hot and cold storage tanks (Table 3). A larger difference on average between the hot and cold storage tanks gives increased thermal density and capacity.

The effect of adding solar heating to the HRL is visible in Fig. 21 for the CTS design and Fig. 23 for the VTS design. For the CTS system, the level of the hot storage tank rises and falls noticeably more than the design without solar. The rise corresponds with daylight hours while the falls relate to night time and the lack of solar heating. The regular cyclic pattern of the hot storage temperature in Fig. 23 for the VTS with solar design is caused by the day/night variations in solar availability. Shorter term variations result from the difference in mixed loop return temperatures from the various heat sources on the HRL. The amplitude of the temperature fluctuations is a function of the amount of hot fluid returned compared to the amount of hot fluid in storage.

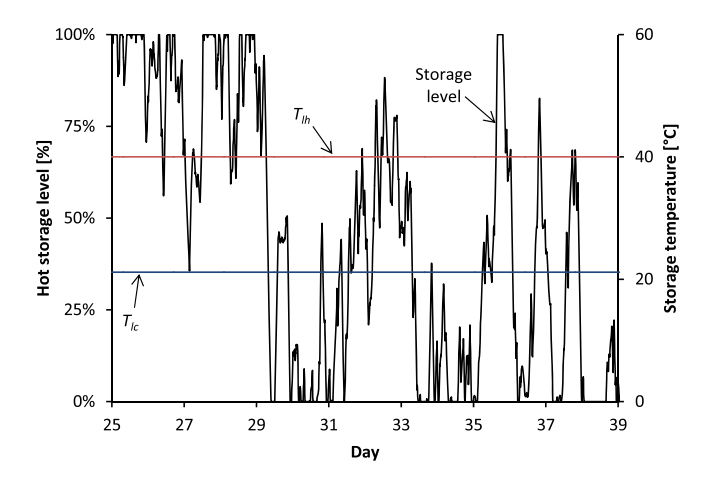


Fig. 20. Thermal storage dynamics for CTS design using 500 m^3 hot and cold storage tanks.

In contrast to the variable hot storage temperature, the cold storage temperature is fairly constant. Many of the sinks at the dairy factory are vital streams for the on-going site operation. These sinks include site hot water, which is constantly being used for washing, and milk treatment streams, which is a necessary process for treating the milk before it is processed into final products. The difference in supply temperature between the sinks is also small ($10-16\,^{\circ}\text{C}$).

The actual combined heat recovery and solar heating with 500 m³ storage tanks are about 5% less than the targeted values as shown in Table 4. The difference between these two values is a loss that can be attributed to three areas: (1) insufficient heat storage, (2) flow rate variability, and (3) temperature variability. These root causes for the drop in performance of the HRL compared to the targets is analysed in the next three sections.

5.2. Effect of storage volume on HRL performance

HRL performance has been modelled for storage capacities between 0 and 1000 m³ (Fig. 24) as well as the case of infinite storage capacity. HRL performance is characterised by the combination of heat recovery and solar heating that replaces the need for steam and hot water utility. With minimal storage the HRL system recovers a high percentage (92–94%) of the heat recovery for the same design method with infinite storage. Issues relating to stream variability and availability on the required storage appear to be

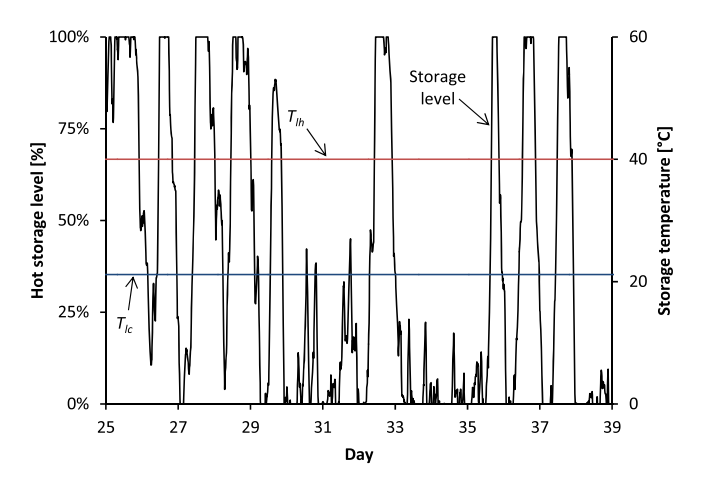


Fig. 21. Thermal storage dynamics for CTS with solar heating design using 500 m³ hot and cold storage tanks.

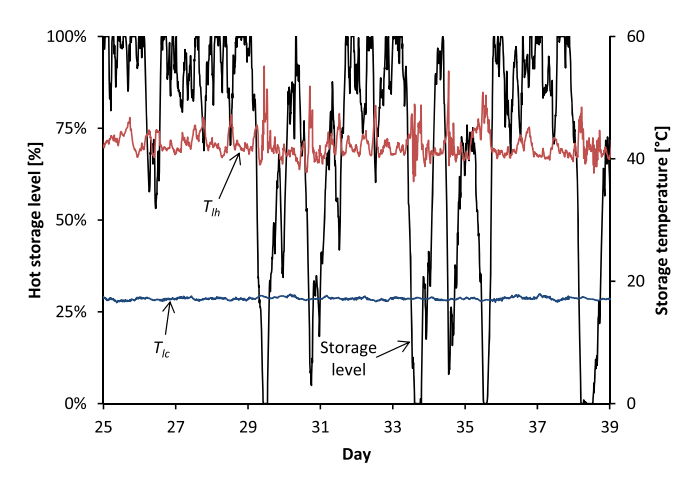


Fig. 22. Thermal storage dynamics for VTS design using 500 m³ hot and cold storage tanks

minimised by a number of sources and sinks on the HRL. As more sinks and sources are connected to the HRL degree of source to sink imbalance is reduced lessening the storage requirement. If there were only one source stream and one sink stream in the HRL, then the system would be out of balance whenever one stream is on while the other is off. But when an HRL system has multiple source/sink streams, the degree of imbalance is dampened by the fact the load is spread across more streams.

Actual HRL performance for an effective thermal storage volume may also be characterised as a percentage of the HRL performance with infinite storage (Fig. 25). The VTS designs require much less storage volume to achieve the same HRL performance percentage as the CTS designs. The effective thermal storage energy densities in the VTS systems are higher due to a larger average temperature difference between hot and cold storage temperatures (Table 3).

5.3. Effect of off-design process flow rates on heat recovery

As the process stream's flow rate changes, a simple feedback temperature control loop is used to adjust the flow rate of the loop to maintain a constant outlet (return) temperature of the loop fluid. When the process stream's flow rate is above its design value, the heat transfer film coefficients increase due to higher Reynolds numbers for the two fluids exchanging heat. This results in an increased pressure drop and log-mean temperature difference due to a larger approach temperature. The duty of the exchanger is now

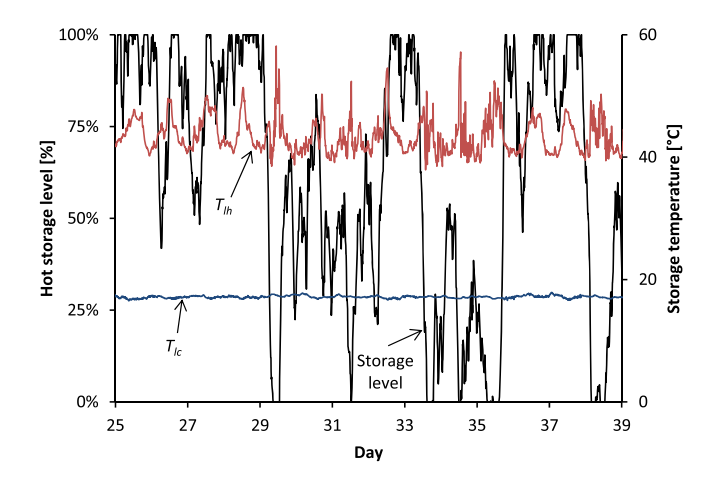


Fig. 23. Thermal storage dynamics for VTS with solar heating design using 500 m³ hot and cold storage tanks.

Table 3Average hot and cold storage temperatures and the associated impact on thermal storage density and capacity.

Design	Average T _{lh} [°C]	Average T _{lc} [°C]	$T_{ m lh} - T_{ m lc}$ [°C]	Thermal storage density increase
CTS	40.0	21.2	18.8	_
CTS with solar	40.0	21.2	18.8	_
VTS	43.3	17.1	26.2	39%
VTS with solar	44.6	17.1	27.5	46%

greater than the design duty, although at the expense of increased pumping power. When the process stream's flow rate is below the design value, *h*, *U*, pressure drop and the log-mean temperature difference are decreased giving a reduced duty.

Fig. 26 plots the actual heat exchanger duty against the heat capacity flow rate of whey B (sink) using the CTS approach. The CTS design is analysed to remove any temperature variability effects. For whey B the supply temperature is an assumed value and is constant for the entire analyse period. The difference between the actual points and the dashed diagonal line (n=1.00, Eq. (10)) represents the duty loss/gain caused by variable whey B flow rates. The average actual duty was 117 kW while the time average targeted duty was 125 kW.

The degree to which the exchanger is above and below the targeted duty (diagonal line) is dependent on the *n* exponent in Eq. (10). The maximum value of n is unity. As n approaches unity, an increase or decrease in C above the design C of the process stream results in a proportional increase or decrease in U and a proportional increase or decrease in Q. As a result there is no reduction in temperature effectiveness based on the process stream with transient C values for n approaching unity as shown in Fig. 27. This implies an important, and perhaps obvious result, that overall heat exchanger performance from transient process streams is always less efficient than from steady process streams with the same time average flow rate and heat exchanger area because n is always significantly less than one in practice. Fig. 27 also shows that temperature effectiveness increases as the flow rate of the process stream is reduced. In essence, the heat exchanger is oversized for flow rates below the design value and undersized for flow rates above the design value. It may appear that choosing a heat exchanger design with a high exponent n is advantageous. However the improved performance at higher flow rates will always come at the expense of increased pressure drop and pumping power, which has close to a squared relationship with flow rate.

5.4. Effect of process supply temperature variability on heat recovery

The third reason that the actual HRL performance is lower than the target is temperature variability. Fig. 28 plots the temperature

Table 4Comparison of combined heat recovery and solar heating targets to actual modelled performance highlighting the root causes of the difference.

Design	Combined heat solar heating [k	•	Root causes of performance reduction [kW]			
	Target	Actual	Insufficient heat storage	Flow rate variability	Temperature variability	
CTS CTS with	, ,	7,872 (94.7%) 8,624 (94.1%)	, ,	` ,	` ,	
VTS	11,347 (100.0%) 12,345 (100.0%)	,	, ,	` ,	` ,	

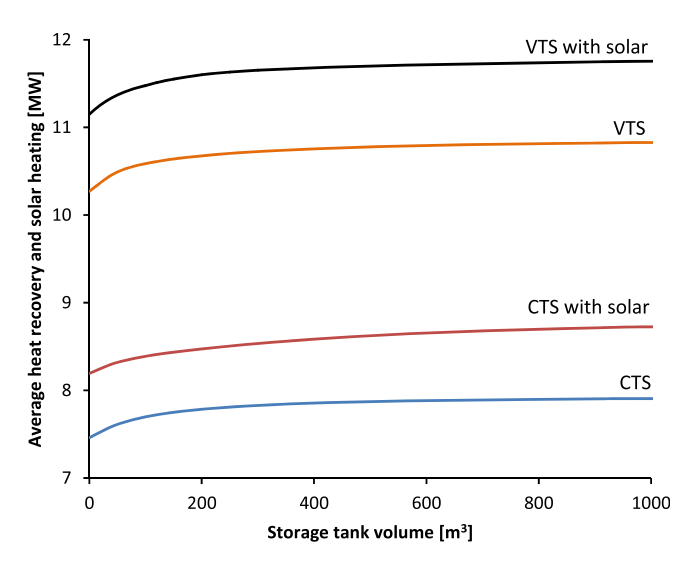


Fig. 24. Effect of thermal storage volume on HRL performance.

effectiveness of the SHW (site hot water) heat exchanger against its inlet temperature. The CTS design is applied to illustrate the effect of process supply temperature variability on heat recovery, which ensures the supply and return temperatures of the HRL are constant. SHW is selected to demonstrate the effect of temperature variability because its inlet temperature is recorded and is known to fluctuate due to changing outside weather conditions as previously shown in Fig. 7.

When the inlet temperature of SHW is less than the loop return set point temperature, the temperature effectiveness of the heat exchanger has some scatter. This scatter is caused by the fact the flow rate of the stream also has variability. To decouple the effects of flow rate variability and temperature variability, exponent n is set to unity eliminating the effect of flow rate variability from temperature effectiveness as shown by the solid line. Low SHW inlet temperatures have high effectiveness and increased duty, whereas high inlet temperatures have low effectiveness and low duties. At times the actual effectiveness and heat exchanger duty

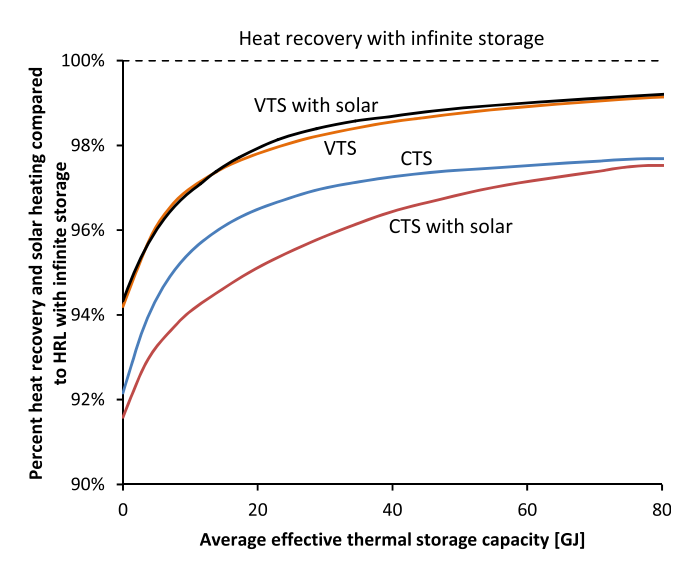


Fig. 25. Effect of average thermal storage capacity on HRL performance as a percentage of the HRL performance with infinite storage.

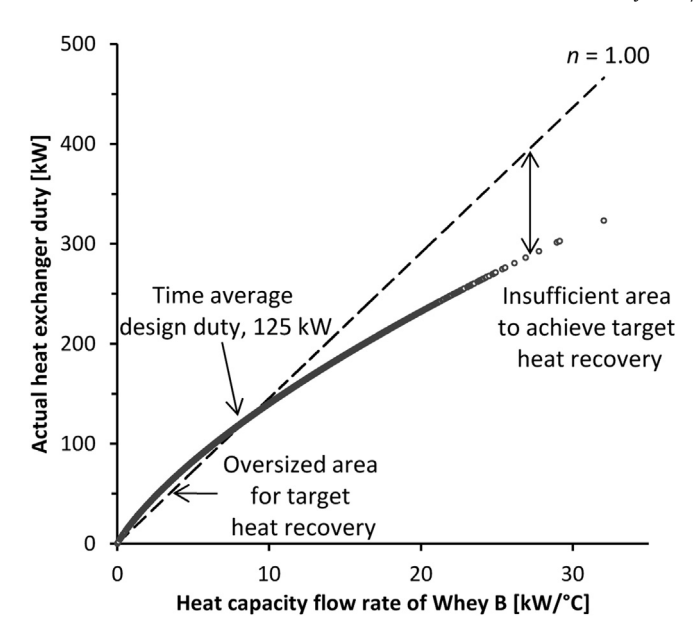


Fig. 26. Actual duty versus heat capacity flow rate of Whey B for CTS design.

are zero because the supply temperature of the process stream exceeds the return temperature set-point of the HRL fluid, which contributes to the amount of decrease HRL performance.

The effect of inlet temperature variability on heat exchanger performance can also be characterised by the outlet temperature of SHW as plotted in Fig. 29. After decoupling the effects of flow rate and temperature variability by setting n to unity, it is noted that the peak outlet temperature of SHW is achieved when the inlet temperature is equal to the design value. This peak outlet temperature is same as the design outlet temperature. The gap between the solid line in Fig. 29 and the design outlet temperature (28.5 °C) represents, therefore, the loss of duty due to inlet temperature variability for the SHW exchanger. However most (90%) of the heat recovery

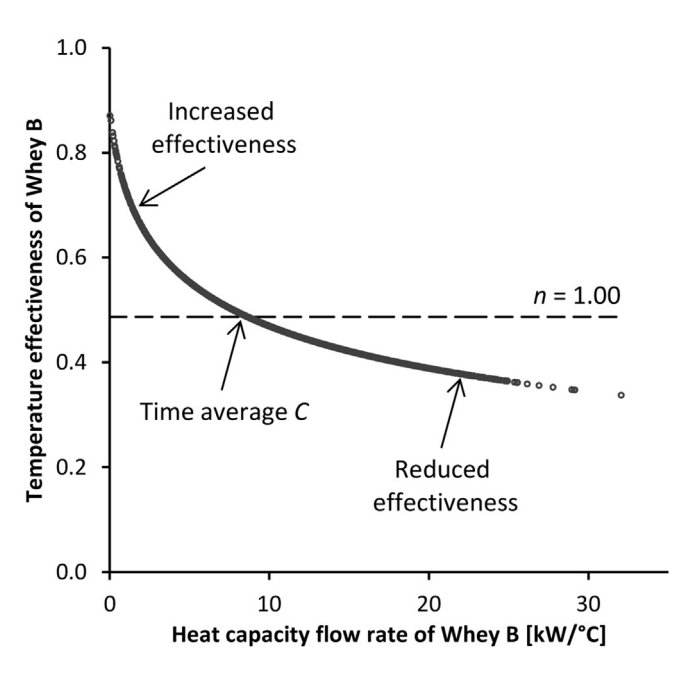


Fig. 27. Temperature effectiveness versus heat capacity flow rate of Whey B for CTS design.

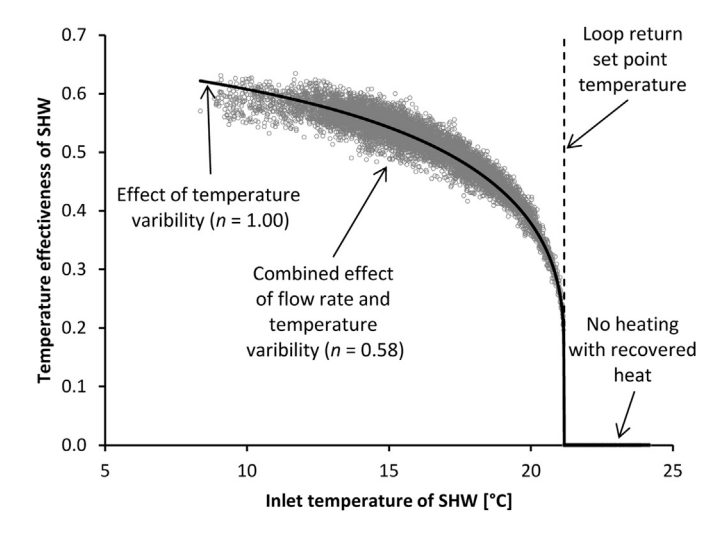


Fig. 28. Temperature effectiveness versus inlet temperature of SHW for CTS design.

loss tied up with the SHW exchanger is the result of high inlet temperatures causing the stream to be incompatible with the operation of the HRL.

5.5. The contribution of dryer exhaust heat recovery and solar heating to improving HRL performance and site energy efficiency

The dairy factory has four milk powder plants. Dryer exhaust heat recovery from these plants contribute about 70% of the heat recovery in the CTS designs and about 50% of the heat recovery in the VTS designs (Table 5). Integrating the dryer exhaust with external operations to the milk powder plant is likely advantageous from a capital cost perspective. Dryer exhaust heat recovery represents the key that is able to unlock a new level of energy efficient dairy processing. Linking exhaust heat recovery into a VTS HRL with the added possibility of solar heating can reduce this site's steam demand by 11.7 MW, which is utility cost savings of \$2.6—\$4.0 million/y.

Future work will look at the control dynamics related to running CTS and VTS HRL's. When a process stream's flow rate changes, its outlet temperature is affected causing control action to take place to restore the desired outlet temperature. The dynamics around a single heat exchanger also contribute to the overall dynamics of the

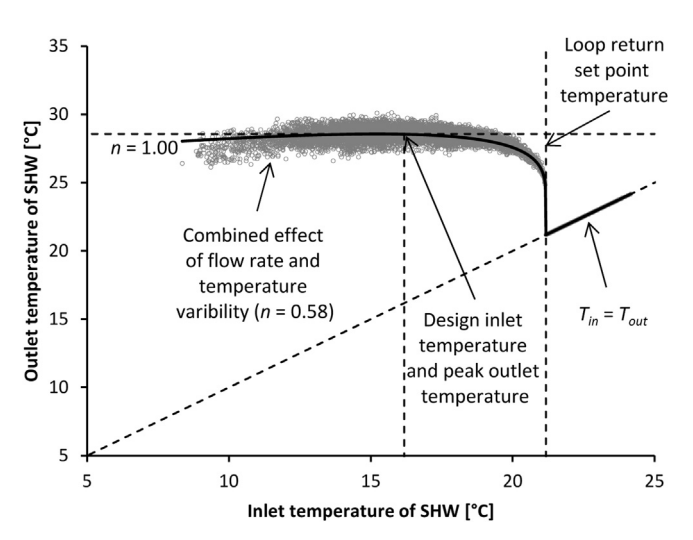


Fig. 29. Outlet temperature versus inlet temperature of SHW for CTS design.

Table 5Contributions to hot utility reduction assuming 500 m³ of storage

Design	Dryer exhaust heat recovery [kW]	Other heat recovery [kW]	Solar heating [kW]	Total [kW]
CTS	5,639	2,233	0	7,872
CTS with solar	5,639	2,134	851	8,624
VTS	5,644	5,134	0	10,777
VTS with solar	5,643	5,139	917	11,700

HRL operation. How these dynamics combine in the heat storage system may prove important for accurately modelling heat recovery.

6. Conclusion

Inter-plant indirect heat integration via an HRL combined with renewable solar heating is potentially an economic method for increasing process energy efficiency in large processing sites with a low pinch temperature. How solar heating is integrated depends on the pinch temperature and the shape of the Composite Curves. Where HRL pinch temperatures are located around the cold storage temperature, solar heating can be directly integrated as an additional source without the need for an additional storage tank.

Compared to the conventional HRL design based on a constant temperature storage system, this new method gives solutions with: (1) more effective distribution of temperature driving forces between heat exchangers resulting in higher $\Delta T_{\rm min}$ values for the same heat recovery, (2) lower average loop flow rates giving reduced pressure drop and pumping requirements, (3) increased average temperature difference between hot and cold storage temperatures increasing thermal storage density and capacity, and (4) requires less thermal storage. The dairy factory analysed lacked sufficient sources. The addition of the dryer exhausts as heat sources was a critical factor in gaining a heat recovery of 10.8 MW for the variable temperature storage design, of which 5.1 MW was contributed from exhaust heat recovery. Solar heating also proved to be a valuable source with the maximum addition of 0.9 MW of heating on average.

References

- Klemeš JJ, Dhole VR, Raissi K, Perry SJ, Puigjaner L. Targeting and design methodology for reduction of fuel, power and CO₂ on total sites. Appl Therm Eng 1997;17:993-1003.
- [2] Rodera H, Bagajewicz MJ. Targeting procedures for energy savings by heat integration across plants. AIChE J 1999;45:1721–42.
- [3] Chen CL, Ciou YJ. Design of indirect heat recovery systems with variable-temperature storage for batch plants. Ind Eng Chem Res 2009; 48:4375–87.
- [4] Kemp IC, Deakin AW. Cascade analysis for energy and process integration of batch processes. Part 1. Calculation of energy targets. Chem Eng Res Des 1989:67:495–509
- [5] Krummenacher P, Favrat D. Indirect and mixed direct-indirect heat integration of batch processes based on pinch analysis. Int J Thermodyn 2001;4: 135–43.
- [6] Morrison AS, Walmsley MRW, Neale JR, Burrell CP, Kamp PJJ. Non-continuous and variable rate processes: optimisation for energy use. Asia Pacific J Chem Eng 2007;2:380-7.
- [7] Walmsley MRW, Atkins MJ, Riley J. Thermocline management of stratified tanks for heat storage. Chem Eng Trans 2009;18:231–6.
- [8] Atkins MJ, Walmsley MRW, Neale JR. The challenge of integrating noncontinuous processes – milk powder plant case study. J Clean Prod 2010;18:927–34.
- [9] Atkins MJ, Walmsley MRW, Neale JR. Process integration between individual plants at a large dairy factory by the application of heat recovery loops and transient stream analysis. J Clean Prod 2012;34:21–8.
- [10] Walmsley MRW, Walmsley TG, Atkins MJ, Neale JR. Area targeting and storage temperature selection for heat recovery loops. Chem Eng Trans 2012;29: 1219–24.
- [11] Walmsley MRW, Walmsley TG, Atkins MJ, Neale JR. Methods for improving heat exchanger area distribution and storage temperature selection in heat recovery loops. Energy 2013;55:15–22.
- [12] Atkins MJ, Walmsley MRW, Morrison AS. Integration of solar thermal for improved energy efficiency in low-temperature-pinch industrial processes. Energy 2010;35:1867–73.
- [13] Nemet A, Klemeš JJ, Varbanov PS, Kravanja Z. Methodology for maximising the use of renewables with variable availability. Energy 2012;44:29–37.
- [14] Klemeš JJ, editor. Handbook of process integration: minimisation of energy and water use, waste and emissions. Cambridge, UK: Woodhead Publishing; 2013
- [15] Walmsley TG, Walmsley MRW, Atkins MJ, Neale JR. Improving energy recovery in milk powder production through soft data optimisation. Appl Therm Eng 2013:61:80–7.
- [16] Kays WM, London AL. Compact heat exchangers. 3rd ed. Malabar, USA: Krieger Pub. Co.; 1998.
- [17] Wang L, Sundén B, Manglik RM. Plate heat exchangers: design, applications and performance. Wit Pr/Computational Mechanics; 2007.
- [18] NIWA. The national climate database; 2013.